Springer

Journal of Mechanical Science and Technology 23 (2009) 3114~3123

Journal of Mechanical Science and Technology

www.springerlink.com/content/1738-494x
DOI 10.1007/s12206-009-0817-2

A study on the measurement of temperature and soot in a constant-volume chamber and a visualized diesel engine using the two-color method †

Yong-taik Han[1], Kyeong-hyeon Lee[2] and Kyoung-doug Min[1,*]

[1]*Department of Mechanical Engineering, Seoul National University, Seoul, 121-742, Korea*
[2]*Interdisciplinary Program in Automotive Engineering, Seoul National University, Seoul, 121-742, Korea*

(Manuscript Received November 12, 2008; Revised June 22, 2009; Accepted July 30, 2009)

Abstract

In this study, the measurements of soot and temperature were used to investigate the turbulent diesel diffusion flame in a constant-volume chamber and a visualized direct injection (D.I.) diesel engine using the two-color method and a high-speed camera. Through these experiments, we effectively acquired information on the temperature and soot by the two-color method in a turbulent diesel diffusion flame. In addition, this experiment revealed that the ***KL*** factor was high on the parts of the chamber where the temperature dropped. On the other hand, the ***KL*** factor was low where the temperature increased rapidly. Also, the highest temperatures of the flame in a constant-volume chamber and in a D.I. diesel engine were approximately 2300K and 2400K, respectively. This study suggests the measurement of not only the temperature but also the soot of a diffusion flame of the diesel engine through an optical methodology.

Keywords**:** Soot; Diffusion flame; Visualized engine; Two-color method; ***KL*** factor; Constant-volume chamber

1. Introduction

Diesel engine designers are challenged by the need to comply with ever more stringent emission standards and at the same time, improve engine efficiency. In order to comply with these more stringent emission standards, which are primarily motivated by environmental concerns, the automotive industry is continuously investigating new ways to improve engine technologies. In recent years, a significant portion of the research in this field has been focused on new combustion modes that will enable reductions in particulate matter and NOx emissions from diesel engines [1, 2].

Furthermore, by understanding the role of combustion in the emissions of NOx, soot, and particulate matter, we can find ways to reduce diesel engine emissions. Many previous studies have concentrated on the study of soot formation. The process of soot evolution from fuel consists of many complex chemical and physical steps, including fuel pyrolysis, polycyclic aromatic hydrocarbon (PAH) formation, particle inception, coagulation, surface growth, carbonization, agglomeration, and oxidation [3-4]. Although soot evolution processes have been previously investigated [5-6], more detailed information on PAHs and soot is still needed to fully understand soot evolution. While soot particle inception is the least understood of these processes, there are still far fewer studies in this area than there are on overall soot formation [7-8]. With respect to the intermediate products of soot particles, studies on the reaction pathway and kinetics of PAHs have made great progress [9], but the precursor particles resulting from PAH growth are still under study.

The conditions and amounts of soot particle generation are functions of pressure, time, air fuel ratio, fuel-type and temperature. The relationships among these parameters are very important for determining

† This paper was recommended for publication in revised form by Associate Editor Kyoung Doug Min

*Corresponding author. Tel.: +82-2-880-1661, Fax.: +82-2-883-0179
E-mail address: kdmin@snu.ac.kr

how to reduce soot particles in the typical flame of a real combustor under high temperature conditions.

For typical exhaust particulate matter consisting of NOx and soot, NOx is generally known to be influenced by temperature such that a high density of NOx is certainly generated in regions of high temperature in modern diesel diffusion flames [10].

Accordingly, high pressure injection techniques have been adopted to reduce soot generation, and ignition delays, and smaller injector nozzles have been used to reduce NOx generation, conditions of which have been researched to relatively induce the homogeneous mixture relatively.

Previous research demonstrated many ways to measure soot and temperature distributions. Matsui et al. [11] applied the two-color method to measure temperature and soot distributions in a diesel engine using visible wavelengths. In addition, Stasio et al. [12] verified that temperature and soot volume fraction values are sensitive to the complex refractive index, m=n-ik. Furthermore, J. Vattulainen et al. [13] developed an application of a double charge-coupled device (CCD) camera system to detect images at two different wavelength bands in a direct-injection diesel engine. In addition, Lee et al. [14] clarified the effect of the injection timing and flame temperature on the generation and extinction of soot using the ***KL*** factor value obtained from the two-color method. However, there have been few studies to measure temperature and soot amount in a real engine. Thus, this study aims to develop temperature and soot measurement techniques for a constant-volume chamber as well as for a diesel engine in turbulent combustion conditions.

2. Experimental apparatus and procedure

2.1 Two-color method theory

The two-color method using soot particles detects the radiation emitted by the particles at two different wavelengths and yields the flame temperature by detecting the unknown quantity of flame emissivity. According to Wien's law, black body emissivity for short wavelengths is defined by Eq. (1), which can be employed to calculate black body emissivity over the visible wavelength range when the temperature is less than 3000K [15],

$$I(\lambda,T)=\varepsilon_\lambda c_1\lambda^{-5}\exp(-\frac{c_2}{\lambda T}) \tag{1}$$

where λ is the wavelength, T is the absolute temperature, c_1 and c_2 are the Planck constants, $c_1 = 3.742 \times 10^8$ w·μ m^4/m^2 and $c_2 = 1.439 \times 10^8$ μm·K, and ε_λ is the short wavelength emissivity of the flame. Eq. (2), known as Lambert Beer's law, is applied to calculate soot temperature using its emissivity,

$$\varepsilon_\lambda = 1-e^{-K_\lambda L} \tag{2}$$

When the scattering rate can be ignored, K_λ becomes the absorbance in Eq. (2). If the soot particle in a diesel flame is applied to the short wavelength emissivity, it becomes $\alpha_\lambda = K/\lambda^\alpha = K_\lambda$ by using the empirical Equation of Hottel and Broughton [16]. In this Equation, K is the absorption coefficient associated with the density of the soot particle, and α is basically determined as a function of particle diameter but can be regarded as a spectral range constant (1.38) [17]. By combining Eq. (2) and $\alpha_\lambda = K/\lambda^\alpha = K_\lambda$, Eq. (3) is obtained as follows

$$\varepsilon_\lambda = 1-\exp(-\frac{KL}{\lambda^\alpha}) \tag{3}$$

This is the approximate value of the strict solution obtained from the scattering theory of small particles, and L is the flame axial geometrical thickness. The product K L is called the ***KL*** factor which is proportional to the soot volume fraction λ^α is the approximate effect of the wavelength, and index α is a function of the particle diameter and soot refractivity. This is dependent on the structure of the flame and the type of fuel. Based on soot density in Eqs. (1) and (2), the value of ***KL*** is generally expressed by the following Equation

$$KL=-\lambda^\alpha \ln[1-\exp(-\frac{c_2}{\lambda}(\frac{1}{T_a}-\frac{1}{T}))] \tag{4}$$

where T_a denotes the flame temperature measured at a certain wavelength. As notated, T_{a1} and T_{a2} mean flame temperature are measured at 550 nm and 750 nm wave length, respectively. Eq. (5) and (6) are derived by dividing Eq. (4) into two separate Equations using the two wavelengths from the two-color method, λ_1 and λ_2.

$$KL=-\lambda_1^\alpha \ln[1-\exp(-\frac{c_2}{\lambda_1}(\frac{1}{T_{a1}}-\frac{1}{T}))] \tag{5}$$

$$KL = -\lambda_2^{\alpha} \ln[1-\exp(-\frac{c_2}{\lambda_2}(\frac{1}{T_{a2}}-\frac{1}{T}))] \quad (6)$$

$$\lambda_1^{\alpha}[1-\exp(-\frac{c_2}{\lambda_1}(\frac{1}{T_{a1}}-\frac{1}{T}))] = \lambda_1^{\alpha}[1-\exp(-\frac{c_2}{\lambda_1}(\frac{1}{T_{a1}}-\frac{1}{T}))] \quad (7)$$

By setting Eqs. (6) and (7) equal to each other, ***KL*** is removed λ_1 and λ_2 can be obtained. Alternatively, ***KL*** can be calculated by measuring T_{a1} and substituting T_{a2}. Radiation from other gases can be ignored because the diesel flame is radiative, and luminous radiation from the soot particle emits a strong continuous spectrum [18].

2.2 Diesel diffusion flame in a constant volume chamber and a visualized diesel engine

2.2.1 Measurement of turbulent diffusion flame using a constant-volume chamber

A turbulent diesel diffusion flame was generated using an injector with a diameter of 0.25 mm and a one-hole nozzle spraying at 1000 bar pressure in a visualized constant-volume chamber. Fig. 1 shows the picture of constant-volume chamber. To generate a diesel diffusion flame, C_2H_2, O_2, and N_2 gas were supplied and ignited using a spark plug such that ambient temperature and ambient pressure were generated prior to igniting the diesel diffusion flame.

2.2.2 Test engine and experimental conditions

In this study, a single cylinder D.I. diesel engine, which has an observation window and piston, was used to visualize soot formation and temperature distribution. Fig. 2 and Fig. 3 show the visualization engine system. This engine system has observation windows around the side of the cylinder, through which a sheet laser can be input across the combustion chamber. In addition, the piston is replaced with a transparent quartz piston to investigate the diffusion flame from the bottom of the cylinder. This system is driven by a DC Motor (22 kW) and can change its injection timing via the fuel control system. Table 1 shows the specifications for this engine system.

The pressure of the common rail is adjustable from 250 bar to 1500 bar by controlling the quantity of air generated in the high-pressure pump. The injector, used in this study, had a 5-hole nozzle with spray angle of 153° and was placed on the axis of the combustion chamber. The system consisted of the high-pressure pump, an injector driver (TDH-3200H, TEMS Co.) and a personal computer to acquire data and pictures.

Table 1. Engine specification.

Bore X Stroke	95 X 95
Compression Ratio	17
Displacement Volume	675 cc

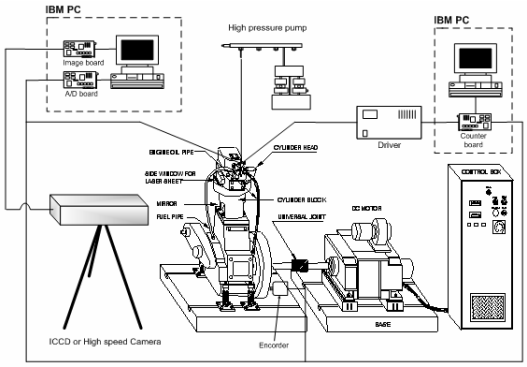

Fig. 2. Schematic of experimental rig for combustion visualization.

Fig. 1. Picture of constant volume combustion chamber.

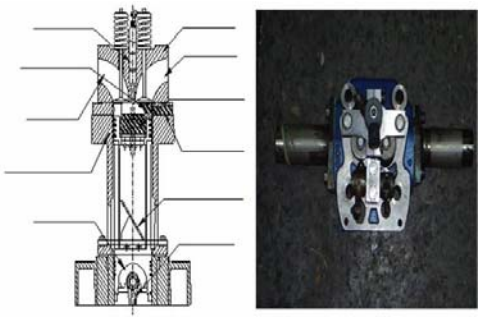

Fig. 3. Cross-section of the visualization engine and the photography of non-swirl type head.

Table 2. Experimental conditions.

Air- fuel ratio	40 : 1
Cylinder head type	Non- swirl head
Injection pressure	300, 600, 900, 1200bar
Engine speed	500, 750rpm

Throughout the experiment, the injection pressure was controlled to be 300, 600, 900 or 1200 bar for the 500 rpm and 750 rpm engine speeds. The amount of supplied fuel was set to a 40:1 air fuel ratio. The timing of a single injection was set before TDC 10^{o} for each condition.

The engine was operated between 85°C and 90°C, which is similar to the coolant temperature of a real engine. The conditions used in this experiment are listed in Table 2.

2.3 Temperature calibration for the two-color method

Before the two-color method can be applied to measure the amount of soot formed and temperature distribution, it is necessary to calibrate the camera for brightness to measure the temperature of the diffusion flame used in the experiment. A standard lamp is used to accurately determine the reference temperature value. In this study, the brightness of the camera was measured according to the temperature of radiation using a highly stable tungsten lamp corrected by a standard verification. The distance between the tungsten lamp and the camera was set at 65 cm, the same measurement distance used in the visualization diesel engine test. The calibration formula can be obtained after the brightness data are stored as a TIFF file from the 8-bit camera (512 x 512 pixels). In this study, the brightness values of two different wavelengths were acquired by using narrow-band filters for 550 nm (FWHM: 10 nm) and 750 nm (FWHM: 10 nm). For application of the two-color method, we used a black-and-white high-speed camera. When a narrow band pass filter is used, the sensitivity of the black-and-white camera becomes much better than that of a color high-speed camera. The camera used had a 1000 fps capture rate, which prevents saturation in front of the 750 nm narrow band pass filter. The intensity of the flame was acquired with both the 550 nm and the 750 nm filter at the same time by using a bi-prism system. The image was acquired using the

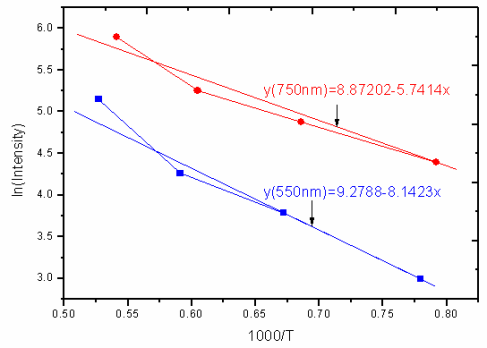

Fig. 4. High-speed camera calibration curve.

550 nm filter on the left side, and the image using the 750 nm filter on the right side.

The temperature of the tungsten lamp applied to calibrate the two-color method is the same as the engine temperatures of 1000, 1200, 1400, 1600 obtained from a black-and-white high-speed camera. From the calibration formula, it could be found that the f-number of the camera lens is inversely proportional to the f-number's square and is also proportional to the shutter speed and the value of the gain. The formula is the same as the value found in Fig. 4, and the temperature could be calculated by a revised linear formula. The camera was set to focus on the top portion of the piston. This position was determined after confirming that there were no problems at a focal depth of 10 mm. If a problem was detected in the visualization process, the camera was installed again and any brightness distortions caused by pollution on the observation window was removed.

The flame data from the D.I. diesel engine was stored in a PC and a program written in Visual C calculated the temperature distribution and the soot density of the observed flame.

3. Experimental results and discussion

3.1 Temperature and soot measurement results for a diffusion flame in a visualized constant-volume chamber

Fig. 5 shows the injected diesel fuel auto-igniting at 1000 bar injection pressure, 1000μ sec injection duration and 3000 fps camera acquisition speed in the visualized combustion chamber.

The fuel, which was injected from the top side, was ignited all the way to the perpendicular bottom and developed into maximum diffusion approximately between 1.333 msec and 1.667 msec.

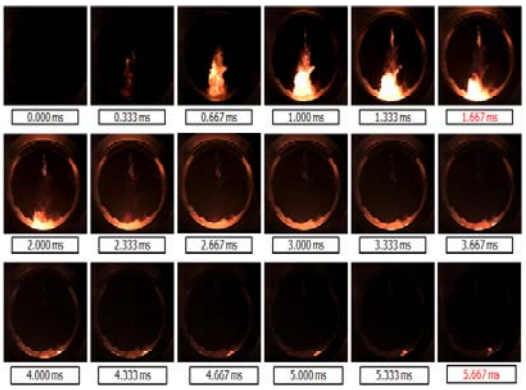

Fig. 5. Flame visualization of a constant volume combustion chamber.

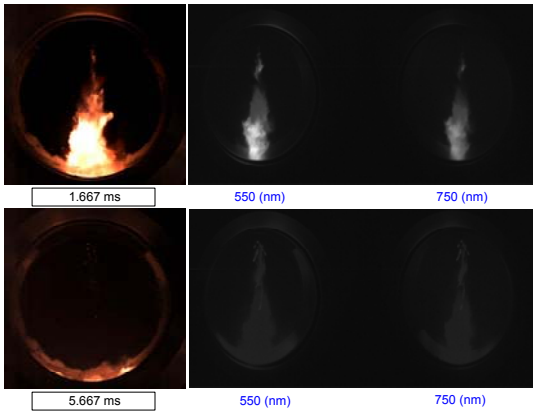

Fig. 6. Photography of raw image acquired by 550nm, 750nm narrow band-pass filters.

Also, at the same time, approximately from 1.333 msec to 1.667 msec, the soot quantity of the flame was measured using the two-color method. During the latter part of the flame formation at approximately 5.667 msec, the soot quantity was analyzed again along with the temperature distribution using the two-color method at the same time.

Fig. 6 shows the black-and-white acquisition image obtained with the use of the 550 nm and 750 nm narrow band pass filters, both at maximum flame (1.667 msec) and minimum flame (5.667 msec), in the visualized constant-volume chamber.

The saturation was prevented from the 750 nm-filtered image by using a 2.62 ND (neutral density) filter to acquire a 550 nm image at the same time.

Fig. 7 shows the results of the qualitative soot amount and the temperature distribution of the maximum flame in the constant-volume chamber, which

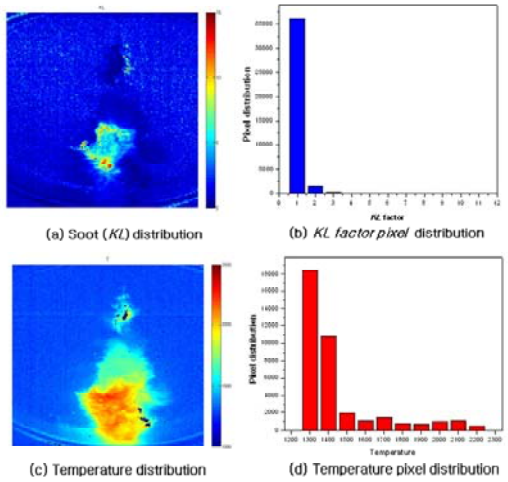

Fig. 7. Soot and temperature distribution acquired by the flame image at 1.667 msec.

were obtained from the two-color method. The maximum amount of soot distribution was observed in the region of greatest flame generation. This suggests that the injected fuel did not fully oxidize in the area where the most diesel fuel was injected. Also, partly maximum soot distribution was shown in the partially lump fuel droplet nozzle tip area. In addition, the maximum temperature was approximately 2300K at the foot of the constant-volume chamber.

Also, (b) and (d) indicate the ***KL*** distribution and temperature distributions from (a) and (c), respectively.

Fig. 8 shows the results for soot distribution and measured temperature 5.667 msec after the injection. Because of the characteristics of the applied nozzle, where clumping fuel droplets are injected during the latter part of the injection, a relatively large amount of soot was observed in another visualization area. The maximum temperature was shown at approximately 1500K and which temperature was 800K below of the maximum temperature. In addition, the extent of the temperature distribution was similar to that of the latter part of the combustion process.

Fig. 9 shows the temperature distribution results of Fig. 5 as the same time sequence using the two-color method. Also, the temperature decreases after the middle phase of the combustion process and the temperature decreases even further in the latter part of combustion process. Furthermore, the maximum temperature is shown in the middle of flame generation development.

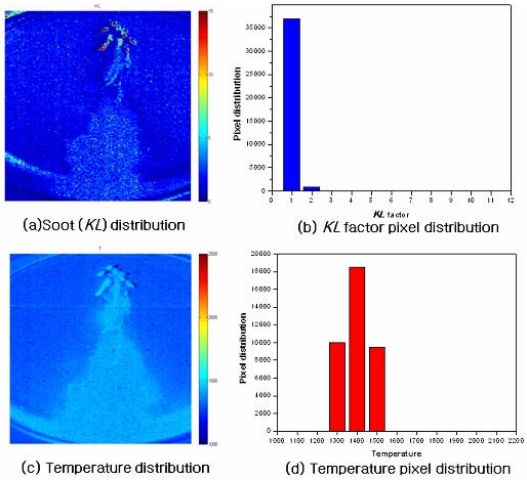

Fig. 8. Soot and temperature distribution acquired by the flame image at 5.667 msec.

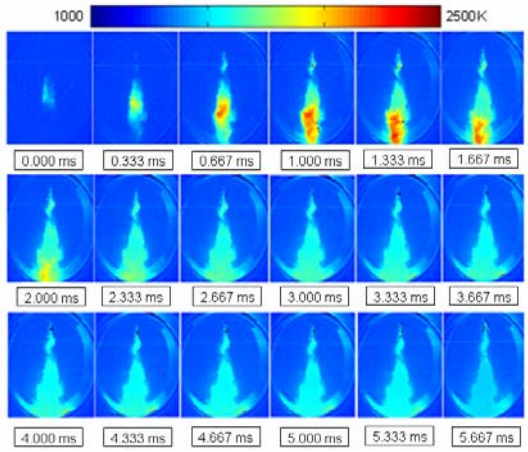

Fig. 9. The results of flame temperature for constant-volume chamber.

Fig. 10 shows the soot distribution results from Fig. 5 as the same time sequence. As the development of flame progresses, we could know that a great amount of soot is created as in Fig. 9, which results from the early part of the flame generation. The timing of soot generation, which is different from the results for temperature generation, is during the latter part of maximum temperature generation, possibly because during the injection of fuel, the flame was generated and oxidized quickly and then the air-fuel ratio changed rapidly during the later phase of flame generation. Also, the time of maximum soot generation was a few msec after maximum temperature generation.

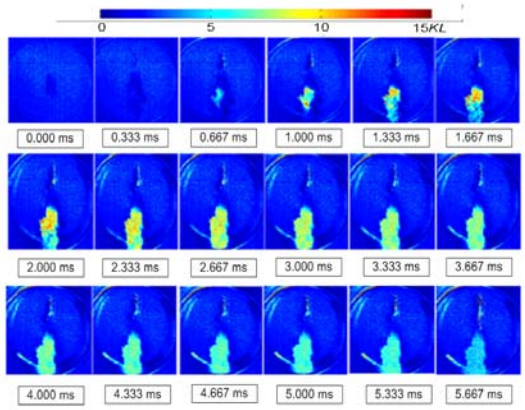

Fig. 10. The results of soot distribution for constant-volume chamber.

3.2 Temperature and soot measurement results for a diffusion flame in the visualized Diesel engine

Fig. 11 shows the results for the visualization of flame distribution and the heat-release rate at 750 rpm engine speed and the different injection pressure in a non-swirl head engine. The higher injection pressure, the shorter the combustion duration and the nearer the maximum flame generation move to the TDC. This tendency was confirmed by the results of the heat-release rate measurement.

This tendency can result from the fact that the higher injection pressure created an increase of turbulence such that the air mixing rate allowed the formation of an advanced premixed flame Also, like this mixing and combustion improvement effect caused an increase of the heat-release rate during premixed combustion at the same time. It is possible that the flame's intensity decreased because the higher injection pressure caused an increase in the premixed flame.

Fig. 12 shows the effect of injection pressure on the maximum temperature distribution for engine speeds of (a) 500 rpm and (b) 750 rpm with a non-swirl head. The fuel injection pressures used in the experiment were 300, 600, 900, and 1200 bar. In this Figure, the maximum temperature is 2100K for an engine speed of 500 rpm and injection pressure of 300 bar, also the maximum temperature is 2300K for same engine speed and injection pressure of 1200 bar. It can be estimated that the real temperature is higher than 2300K because the higher injection pressure increases the air-fuel mixing rate so that the flame intensity declines.

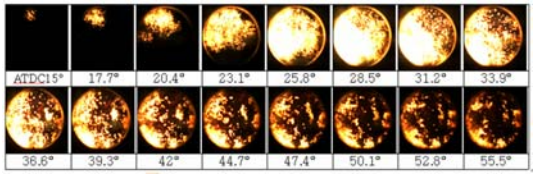

(a) Non-swirl head, 750 rpm, 300 bar

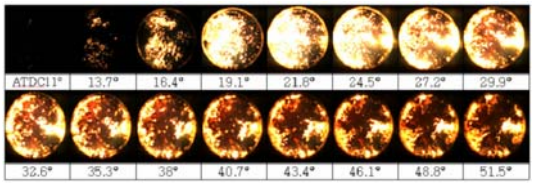

(b) Non-swirl head, 750 rpm, 600 bar

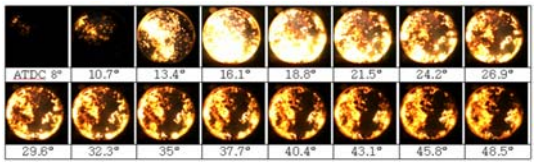

(c) Non-swirl head, 750 rpm, 900bar

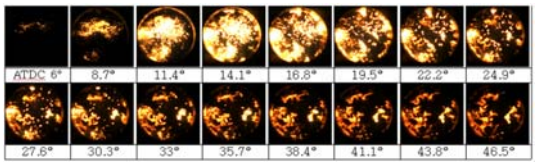

(d) Non-swirl head, 750 rpm, 1200 bar

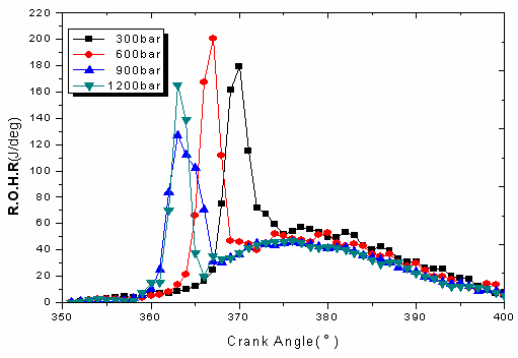

(e) Heat release rate for non-swirl head, 750 rpm

Fig. 11. Comparison of flame visualization and heat release rate with injection pressure.

The maximum temperature is 2300K for an injection pressure of 300 bar and engine speed of 750 rpm, and with the higher injection pressure, the maximum temperature exceeds 2400K. Furthermore, in the case of a 750 rpm engine speed and a 1200 bar injection

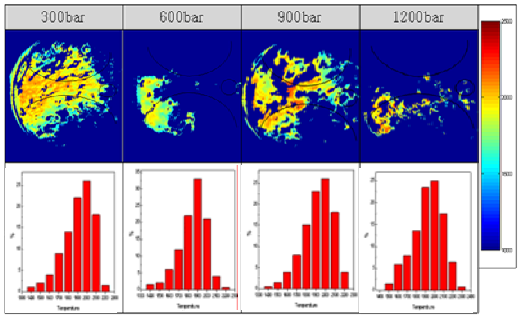

(a) Engine speed (500 rpm)

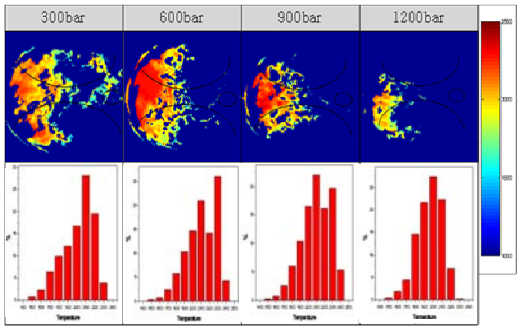

(b) Engine speed (750 rpm)

Fig. 12. Maximum temperature distribution and probability of temperature distribution for non-swirl head at 500 rpm, 750 rpm.

pressure, premixed air-fuel mixing is at a maximum, so that the real temperature could be considered higher than the experimental temperature, such as in the case of a 500 rpm engine speed.

From these results, it could be known that a higher injection pressure increases the air-fuel mixing rate, which in turn increases the burning rate as well as the temperature in the combustor. Correspondingly, higher engine speeds increase the temperature of the diesel combustion flame.

The soot distribution and ***KL*** factor images for engine speeds of (a) 500 rpm and (b) 750 rpm with a non-swirl head are shown in Fig. 13. The fuel injection pressures used in the experiment were 300, 600, 900 and 1200 bar.

As shown in this Figure, the soot was distributed across a wide range for the combustion chamber with a non-swirl head. On the other hand, the soot distribution became narrow at 1200 bar injection pressure because the atomization of the fuel was enhanced. As the fuel injection pressure increased, the ***KL*** factor decreased in the cylinder because the atomization and

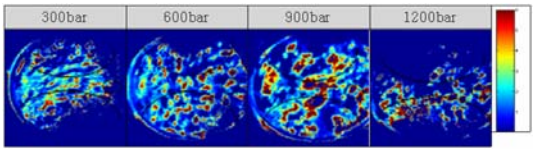

Engine speed (500 rpm)

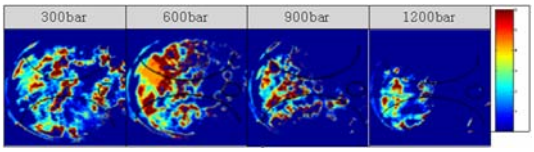

Engine speed (750 rpm)

Fig. 13. Soot distribution and KL factor for non-swirl head at 500 rpm, 750 rpm.

evaporation characteristics of the injected fuel were improved. Combustion temperature increased correspondingly, which an aid in the reduction of emissions. Also, based on the comparison of the temperature distribution results of Fig. 12, the smallest amount of soot distribution was observed in the area of highest temperature, and the greatest amount of soot distribution was observed in the area of lowest temperature.

Fig. 14 shows the temperature distribution in the diesel combustion chamber in terms of crank angle at 500 rpm engine speed and 600 bar injection pressure. As shown in the Figure, the flame initially appeared at ATDC 4° due to an ignition delay, although the injection timing was set at TDC. The flame was fully developed in the whole combustion chamber at ATDC 7°, and the maximum temperature was observed at ATDC 10°. Afterwards, the flame temperature decreased as a result of expansion of the combustion chamber volume during the expansion stroke. In addition, the temperature of the flame in the center of the chamber was over 2300K, and the temperature close to the combustion chamber wall was relatively low. This may be attributed to the heat transfer from the flame to the wall.

Fig. 15 indicates the process of soot generation with an engine speed of 500 rpm and a fuel injection pressure of 600 bar using a non-swirl head, showing the combustion processes of creation, growth, and extinction. These images confirm that flame creation and soot generation exist across the entire area of the combustion chamber. In particular, soot was formed at the end of the flame and on the wall of the combustion chamber. Soot was also generated in the part of flame where the injected fuel impinged on the wall.

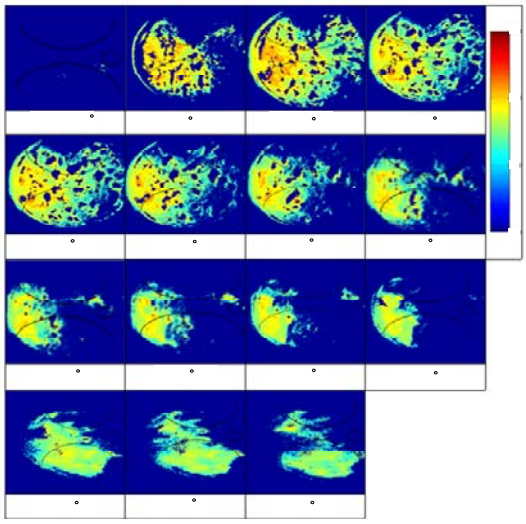

Fig. 14. Flame temperature distribution for non-swirl head at 500 rpm, 600 bar.

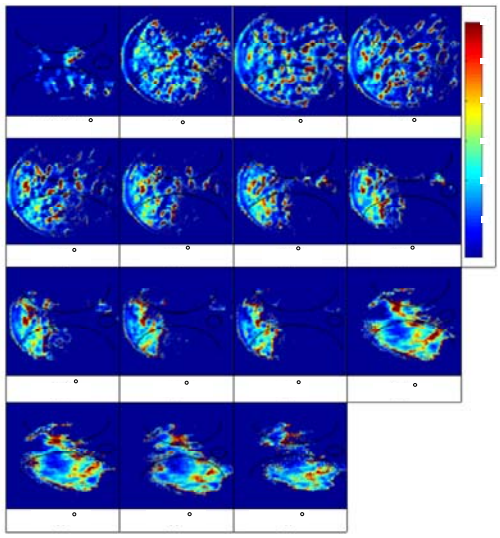

Fig. 15. Soot distribution and KL factor for non-swirl head at 500 rpm, 600 bar.

4. Conclusions

This research investigated the temperature of a diffusion flame and the soot distribution in a constant volume chamber and a D.I. diesel visualization engine by using the two-color method. This is a non-invasive technique that can evaluate combustion temperature and soot formation in a combustion chamber under various conditions. This paper provides a suitable methodology for engineers who need to better understand the physical phenomena involved in diesel

combustion, to aid in their development and design of a more reliable combustor. The main conclusions are as follows:

(1) In this study, maximum soot distribution was generated during the latter part of the maximum flame generation phase, and maximum temperature was observed in the previous phase using a one-hole injector in a constant-volume chamber.

(2) In the case of a diesel diffusion flame, the maximum temperature was observed at 2300K during an early stage of flame development in the middle of the flame. Maximum soot distribution was occurred a few after the maximum temperature was reached.

(3) Higher injection pressure created an increase in turbulence, so that the air mixing rate resulted in an advance premixed flame. The flame's intensity was decreased because of the high injection pressure, thus resulting in an increase of the premixed flame in the visualized D.I. diesel engine.

(4) Finally, the smallest amount of soot distribution was observed in the area of highest temperature and the greatest amount of soot distribution was observed in the area of lowest temperature in the visualized D.I. diesel engine.

Acknowledgment

This work was supported by the second stage of the Brain Korea 21 Project in 2008.

References

[1] R. Barale, M. Bulleri, G. Cornettic and W. F. Wachter, Preliminary Investigation on Genotoxic Potential of Diesel Exhaust, *SAE International* (1992) Paper no. 920397.

[2] J. K. Yeom, Diagnostics of the Behavior Characteristics of the Evaporative Diesel Spray by Using Images Analysis, *J. of Mechanical Science and Technology* 22 (2008) 1785-1792.

[3] D. J. M. Miller and J. B. A. Mitchell, Studies of the Effects of Metallic and Gaseous Addictives in the Control of Soot Formation in Diffusion Flames, *Combustion and Flame* 75 (1989) 45-56.

[4] S. J. Harris and A. M. Weiner, A Picture of Soot Particle Inception, Twenty-Second Symposium on Combustion, The Combustion Institute Pittsburgh (1988) 333.

[5] W. L. Flower and C. T. Bowman, Soot Production in Axisymmetric Laminar Diffusion Flames at Pressures from One to Ten Atmosphere, Twenty-first Symposium on Combustion The Combustion Institute Pittsburgh (1986) 1115-1124.

[6] P. A, Bonczyk, Supression of Soot in Flame by Alkaline-Earth and Other Metal Addictives, *Combustion Science and Technology* 59 (1988) 143-163.

[7] L. Warnatz, The Structure of Laminar Alkane-, Alkene-, and Acethylene Flames, Eighteenth Symposium on Combustion The Combustion Institute Pittsburgh (1981) 369.

[8] C. K. Law, Dilution and Temperature Effect of Inert Addition on Soot Formation in Counterflow Diffusion Flames, *Combustion Science and Technology* 61 (1988) 51-73.

[9] W. N. Lee, The Effect of Pressure on PAH and Soot Formation in Laminar Diffusion Flames, *The Korean Society of Mechanical Engineers* 22 (10) (1998) 1445-1453.

[10] J. E. Dec, A Conceptual model of D. I. diesel combustion based on laser-sheet imaging, *SAE International* (1997) Paper no.970873.

[11] M. Yukio, K. Takeyuki and M. Shin, A Study on the Time and Space Resolved Measurement of Flame Temperature a Soot Concentration in a D.I. Diesel Engine by the Two-Color Method, *SAE International* (1979) Paper no.790491.

[12] S. d. Stasio and P. Massoli, Influence of the Soot Property Uncertainties in Temperature and Volume-fraction Measurements by Two-color Method, *Measurement Science and Technology* 5 (1994) 1453-1465.

[13] J. Vattulainen, V. Nummela, R. Hernberg and J. Kytola, A System for Quantitative Imaging Diagnostics and Its Application to Pyrometric In-cylinder Flame-temperature Measurements in Large Diesel Engines, *Measurements Science and Technology* 11 (2000) 103-119.

[14] T. W. Lee, S. B. Lee and J. R. Ha, A Study on a Technique of the Measurements of Flame and Soot Using the Two-color Method in Diesel Engines, *The Korean Society of Mechanical Engineers* 20 (1996) 550-556.

[15] X. He, X. Ma, F. Wu, J. Wang and S. Shuai, Investigation of Soot Formation in Laminar Diesel Diffusion Flame by Two-Color Laser-Induced Incandescence, *SAE International* (2008) Paper no. 2008-01-1064.

[16] H. Hottel and F. Broughton, Determination of True Temperature and Total Radiation from Luminous Gas Flames, *Industrial and Engineering*

Chemistry Analytical Edition 4 (1932) 166-175.

[17] H. Zhao and N. Ladommatos, Optical Diagnostics for Soot and Temperature Measurement in Diesel Engines, Prog. *Energy Combust. Sci.* 24 (1998) 221-255.

[18] M. Grunwald, Two-dimensional Flame Temperature Measurements of Diesel Combustion Using the Two-Color Method, M. S. Thesis, Mechanical Engineering Department University of Wisconsin-Madison (1994).

Kyoungdoug Min received his B.S. and M.S. degrees from the Department of Mechanical Engineering at Seoul National University in 1986 and 1988, respectively. He then obtained his Ph.D. degree from M.I.T. in 1994. He is currently a professor in the school of Mechanical and Aerospace Engineering at Seoul National University.

Yong-taik Han received his B.S, M.S and Ph.D. degrees from the Department of Mechanical Engineering at Hanyang University at 1995, 2000, and 2006. He is currently a post doctor in the schoo of Mechanical and Aerospace Engineering at Seoul National University.